STM JOURNALS

Journal of
Polymer & Composites

ISSN: 2321-2810 (Online)
ISSN: 2321-8525 (Print)
Volume 11, Special Issue 11, 2023
DOI (Journal): 10.37591/JoPC

http://engineeringjournals.stmjournals.in/index.php/JoPC/index

Research JoPC

Dielectric Properties of Reduced Graphene Oxide with Nickel Cobalt Ferrite and Nickel Zinc Ferrite Epoxy Nanocomposites

Manuel George[1,*], P.P. George[2]

Abstract

In this work, two systems of the composite were prepared using NiCoFe and NiZnFe with reduced graphene oxide(rGO) epoxy and the samples were subjected to electrochemical impedance spectroscopy (EIS). The Quality factor and loss tangent values of the composite was found out as a function of frequency. The modified ferrite-graphene-epoxy blends show dielectric loss and Quality factor values at low frequency. The incorporation of graphene aims to improve electrical conductivity, while the magnetic nanoparticles contribute to enhanced dielectric permittivity. The fabrication process involves the dispersion of these nanofillers within the epoxy matrix, followed by thorough characterization of the resulting nanocomposites using techniques such as impedance spectroscopy and scanning electron microscopy. NiZnFe-rGO obtained higher Quality factor in the intermediate concentration at higher frequencies but the loss tangent obtained least in the higher frequency range. The dielectric loss was least with NiCoFe-rGO which is due to the decrease of grain size at the same time dielectric loss was high for NiZnFe-rGO. Thus, a synergistic effect obtained with multifunctional fillers on the dielectric constant, dielectric loss, and electrical conductivity of the nanocomposites. The study aims to provide insights into the tailored design of advanced dielectric materials for applications in electronic devices, capacitors, and electromagnetic shielding, exploiting the unique properties of graphene and magnetic nanoparticles in epoxy nanocomposites.

Keywords: Quality factor, dielectric constant, loss tangent, frequency range, graphene, epoxy.

INTRODUCTION

Due to its covalent bond and insulating properties, the polymer specifically epoxies won't play any part in ion conduction. Electronics have employed epoxy blends with conducting fillers as coating materials, embedding materials, and dielectric compounds [1, 2]. There happens an interaction between the conducting filler and the epoxy polymer blends [3]. These interactions would depend on the concentration of fillers and the mixing protocol and hence affect the conductivity of the polymer [4]. Ni–Zn ferrite, were developed for the applications where high permeability and low loss were the main requirements. High concentration (50 wt%) of micro filler particles causes the insulation problems such as increased dielectric loss and decreased breakdown strength and improved the resistance with less amount [5, 6, 7].

Under high frequency and high voltage electric fields, epoxy's low dielectric constant reduces electrical coupling, reduces signal distortion, and has low dielectric loss and strong breakdown strength. These properties assure dependable

***Author for Correspondence**
Manuel George

[1]Associate Professor, Department of Mechanical Engineering, Mangalam College of Engineering, Ettumanoor, Kerala, India
[2]Professor, Department of Basic Sciences, Mangalam College of Engineering, Ettumanoor, Kerala, India

Received Date: December 05, 2023
Accepted Date: January 29, 2024
Published Date: April 02, 2024

Citation: Manuel George, P.P. George. Dielectric Properties of Reduced Graphene Oxide with Nickel Cobalt Ferrite and Nickel Zinc Ferrite Epoxy Nanocomposites. Journal of Polymer & Composites. 2023; 11(Special Issue 11): S28–S37.

operations and lengthen the service life of equipment [6]. Due to the high dielectric constant, conducting polymers and Poly(vinyl alcohol) blend systems loaded with various weight fractions of graphene oxide are used for wearable electronics [6]. In polymer nanodielectric composites, enhanced polarisation results from the voluntary polarisation of nanofillers by the applied external field across a nanoscale [7, 8]. Partial electrical discharges were resisted by a fluid diglycidyl ether of bisphenol A (DGEBA)/methyl hydride epoxy system that was also loaded with inorganic particles.

Due to the useage of shrinked size electronic devices, dielectric materials with a high value of dielectric constant have recently attracted a lot of attention [9]. It is perfect for microwave dielectric applications, such as filters and resonators, due to the low dielectric loss (tan d) and high permittivity [10, 11]. With decreasing filler size, the matrix filler interface has a considerable impact on the permittivity, conductivity, electromechanical, and optical characteristics [12]. According to Hallouet B [13], the inherent dielectric strength of nanocomposites increases according to the volume percentage of nanoparticles. However, the matrix polymer behaves like a bulk material in micro-composites. With higher concentrations and smaller particle sizes, the total contact area rises, changing the polymer's structure. This changed the molecule polarizability-related interactions at the particle-matrix interfaces [13].

Sabu, M. et al. [14] reported that the dielectric response of the composites may increase or decrease by the following mechanism: firstly, the dipole molecular chains inside the polymer have more ability to move at frequency and the expansion of cured epoxy will destroy the connections between filler particles and epoxy, which should result in a reduction in the dielectric constant.

Cheng, Y. et al. [15] proposed that nanocomposites exhibit a high dielectric strength, whereas microcomposites exhibit a high thermal conductivity. With an increase in frequency, due to the sufficient time taken for interfacial polarization thereby obtaining a decrease in the dielectric constant. Zhang, X. [16] reported that nano-ZnO composites in lower concentration than the micro-ZnO composites, limits enhancement in dielectric and piezoelectric responses.

So, the purpose of the present work is to gain knowledge into the dielectric properties of both NiCoFe and NiZnFe with graphene in epoxy by plotting the dielectric constant and loss as a function of frequency.

EXPERIMENTAL

Materials

99.8% pure graphite flakes was received from Alfa Asear, concentrated sulfuric acid (H_2SO_4), phosphoric acid (H_3PO_4), hydrochloric acid (HCl), hydrogen peroxide (H_2O_2), potassium permanganate ($KMnO_4$), ethanol, N, N dimethylformamide (DMF) Nickel nitrate, cobalt nitrate, ferric nitrate of analytical grade obtained from S. D. Fine chemicals, India. Polyvinylpyrrolidone (PVP) *M* w ~ 10,000 was obtained from Sigma Aldrich, India.

Preparation of Reduced Graphene oxide (rGO)

Graphene oxide synthesized by modified Hummers method [17]. Reduced Graphene oxide (rGO) was synthesized by solvothermal reduction method [18]. Initially, 1 mg/ml PVP (polyvinylpyrrolidone) was dissolved in DMF using magnetic stirring. Thereafter the solution turns into a homogenous mixture followed by addition of 1 mg/ml graphene oxide added probe sonicated for 1 h. The solution was fetched to Teflon lined stainless steel autoclave and heated at 180°C for 8 h. The constituents were washed repeatedly with distilled water and ethanol several times and dried in vacuum oven at 60 °C for 48 h to obtain a fine powder of reduced graphene. Nickel zinc ferrite and nickel cobalt ferrite was synthesized by coprecipitation method [19, 20]. Suitable concentration of Nickel nitrate, zinc nitrate and ferrous nitrate were taken and dissolved in deionized water followed by addition of the NaOH into that to

maintain the pH=12. Then the precipitate was washed with Distilled water and ethanol. The precipitate was kept in oven and dried at 60°C for 12 hrs. The same protocol was adopted for nickel cobalt ferrite.

Transmission Electron Microscope (TEM)

TEM image of solvothermally reduced graphene oxide (rGO) shown in Figure 1(a) and the SAED is shown in Figure 1(b).

X-ray Diffraction (XRD)

NiCoFe nanocrystals achieved interplanar spacings of 0.239 nm, which correspond to the (311) crystal planes [21] from the XRD plots (Figure 2), while NiZnFe nanocrystals obtained interplanar spacings of 0.256 nm, which correspond to the (311) crystal planes. Peaks at 2Θ of 30◦, 35◦, 43◦, 56.94◦, 62.56◦ related to XRD diffraction planes (2 2 0), (3 1 1), (4 0 0), (5 1 1), (4 4 0), confirmed that cubic spinel nickel–zinc ferrite (JCPDS 08-0234) [22]. Peaks indexed at 35◦, 43◦, 56◦, 62◦ mapped to the (3 1 1), (4 0 0), (5 1 1) and (4 4 0) lattice planes of the cubic unit cell, indicating the formation of a single-phase cubic spinel nickel–cobalt ferrite (JCPDS 22-1012) [23].

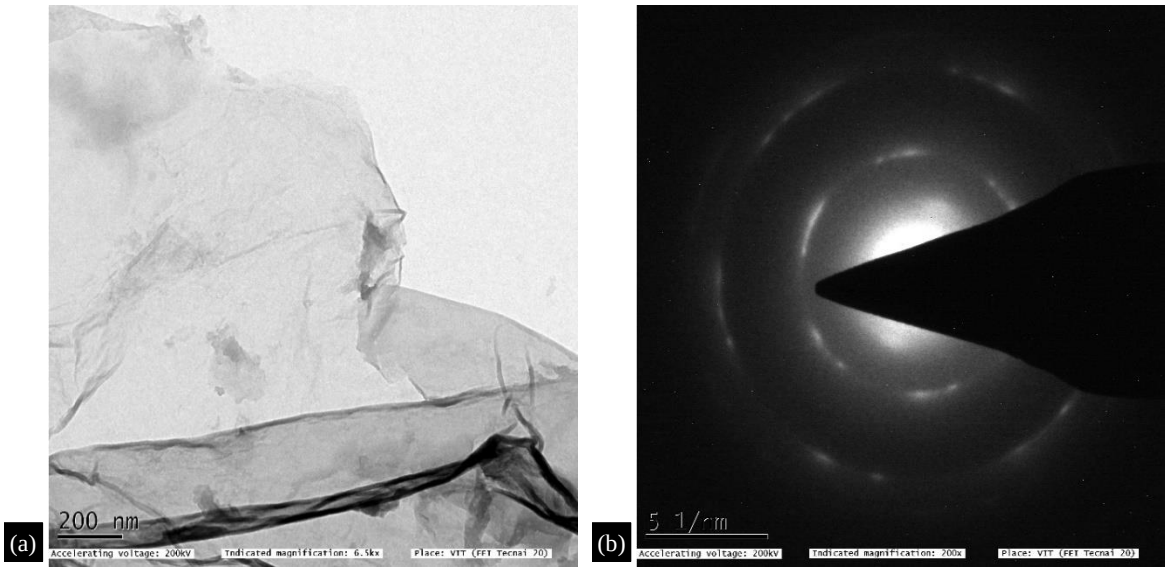

Figure 1. (a) TEM image of reduced graphene oxide (rGO) (b) SAED image of reduced graphene oxide (rGO).

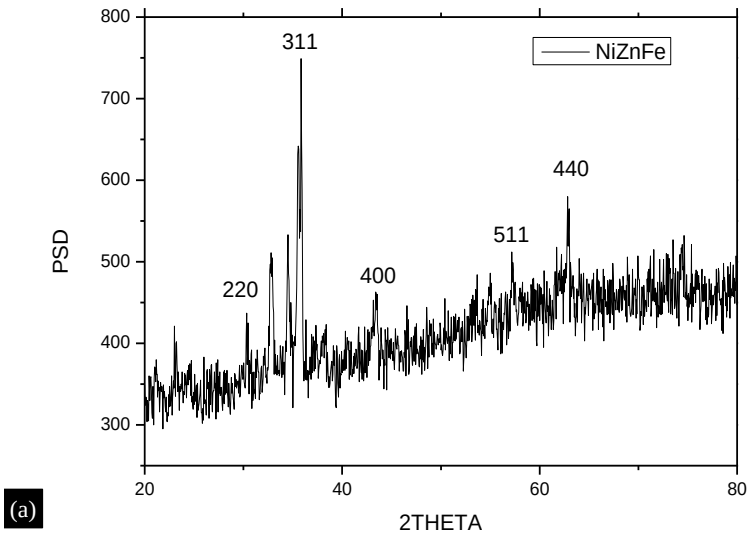

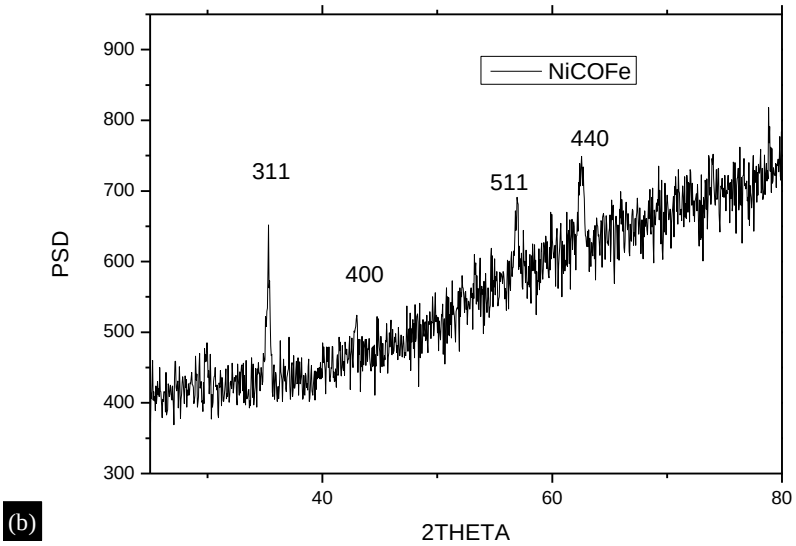

Figure 2. XRD plot of (a) NiZnFe, (b) NiCoFe.

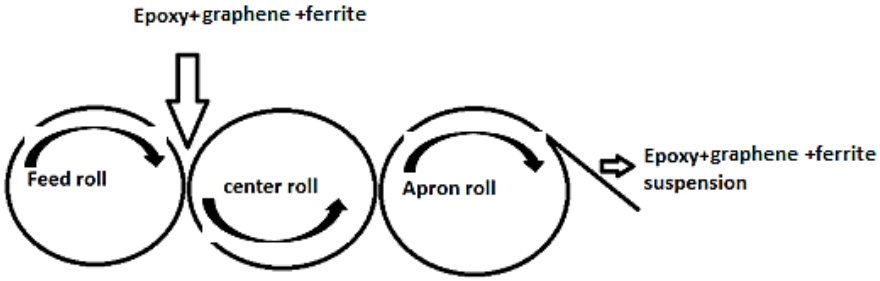

Figure 3. Schematic of preparation of composite on 3 roll mill

Synthesis of Graphene/Ferrite/Epoxy Nanocomposites

A desired weight percentage of reduced graphene oxide (rGO) and NiCo Ferrite was added in 20 gm of epoxy. Further, this solution was added into 3 roll mill as shown in the schematic diagram Figure 3. Thereafter, the mixture was taken out and added the required amount of hardener. Thereafter, the mixture was open casted into the desired mould of ASTM standard and cured at room temperature for 24 h. The convalescented epoxy nanocomposites were post-cured at 70°C for 24 hrs in hot air oven. The same procedure is adopted for NiZn Ferrite. Table 1 and 3 denotes the various concentrations of samples prepared with rGO with NiZnFe and NiCoFe.

RESULT AND DISCUSSION

The Quality, Q factor, is the ratio of the material's initial energy stored to energy lost in one radian of oscillation. The ratio of the imaginary to the real part of the dielectric constant is known as the loss tangent, or tanδ. It refers to the quantitative loss of electrical energy resulting from a variety of physical processes, including dielectric relaxation and resonance, and loss from non-linear processes [24]. The Q factor and tan δ spectra of the NiCoFe and NiZnFe in various concentrations with rGO are shown in Figures 4, 5 and Figures 6, 7.

From the impedance spectroscopy, the reduced graphene-ferrite blend system possessed a higher dielectric constant. The general dielectric spectra for all concentrations, the tan δ and Q factors exhibit frequency dependence. All of the samples' acquired Q factor (Figure 5 & 7) and tan δ (Figures 4 & 6) values are found in the low-frequency realm, where they gradually decrease as they approach the high-frequency zone. It results from the dipoles in the polymer blends relaxing [25, 26]. Due to the inability of these dipoles to follow the incoming frequencies at high frequencies, the values are drastically decreasing [27].

Table 1. NiCoFe with rGO

Sample	Epoxy (wt %)	NiCoFe (wt %)	rGO (wt %)
1	20	0.8	0.2
2	20	0.6	0.4
3	20	0.4	0.6
4	20	0.2	0.8

Table 2. Average values of Q factor, tandelta and dielectric const. of NiCoFe-rGO epoxy composite

NiCoFe-rGO	Q factor	tandelta	% decrease in dielectric loss	Dielectric constant	% increase in dielectric const.
sample 1	566.1284	0.009633	-64.99%	16057069.51	79.78%
sample 2	216.7725	0.021225	-22.86%	4265013390	99.92%
sample 3	658.8598	0.73431	96.25%	64626798	94.97%
sample 4	576.9206	0.008207	-70.17%	58276418.52	94.43%
Neat epoxy	426.7927	0.027518		3245277.084	

Table 3. NiZnFe with rGO.

Sample	Epoxy (wt. %)	NiZnFe (wt. %)	rGO (wt. %)
1	20	0.8	0.2
2	20	0.6	0.4
3	20	0.4	0.6
4	20	0.2	0.8

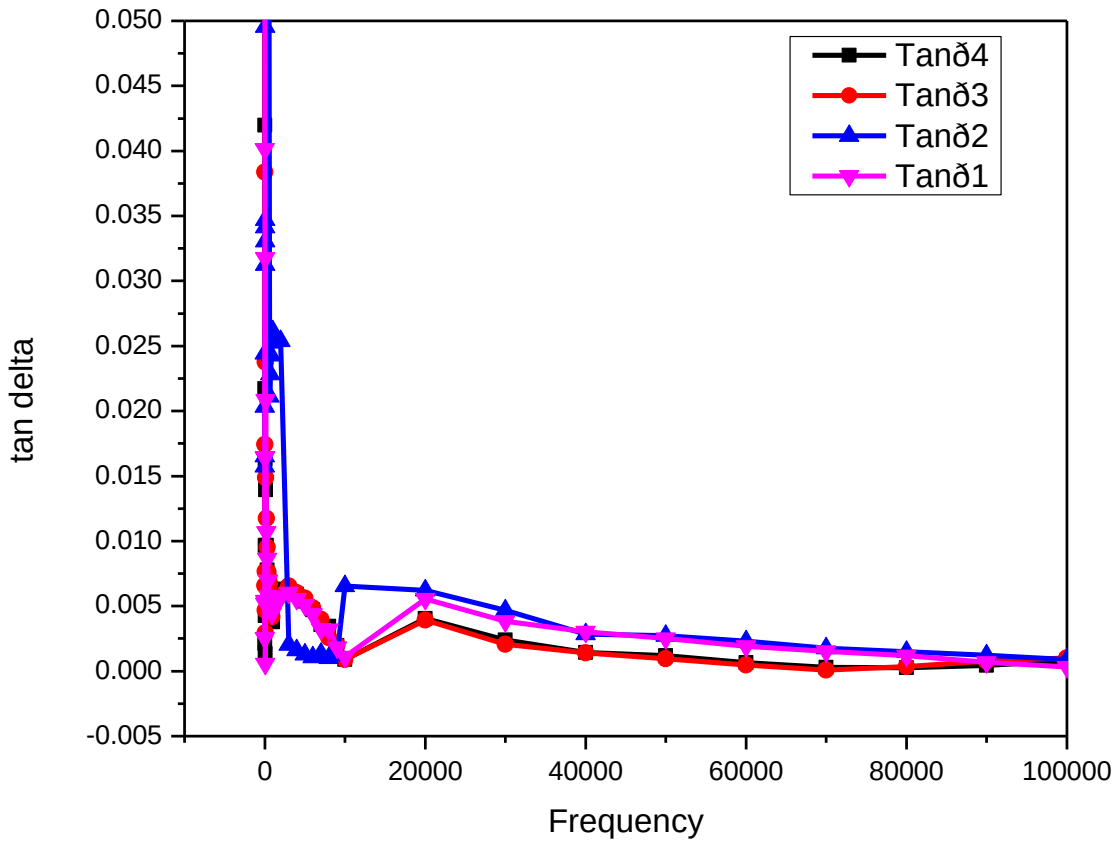

Figure 4. Tandelta for NiCoFe with rGO.

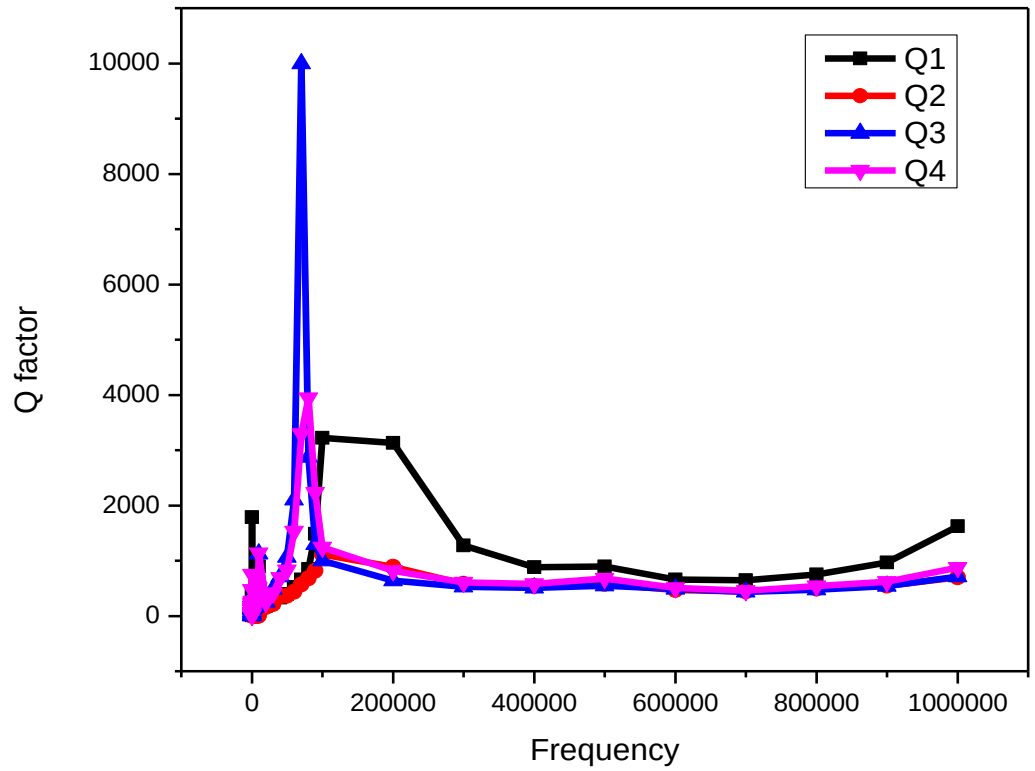

Figure 5. Q factor Vs Frequency for NiCoFe with rGO.

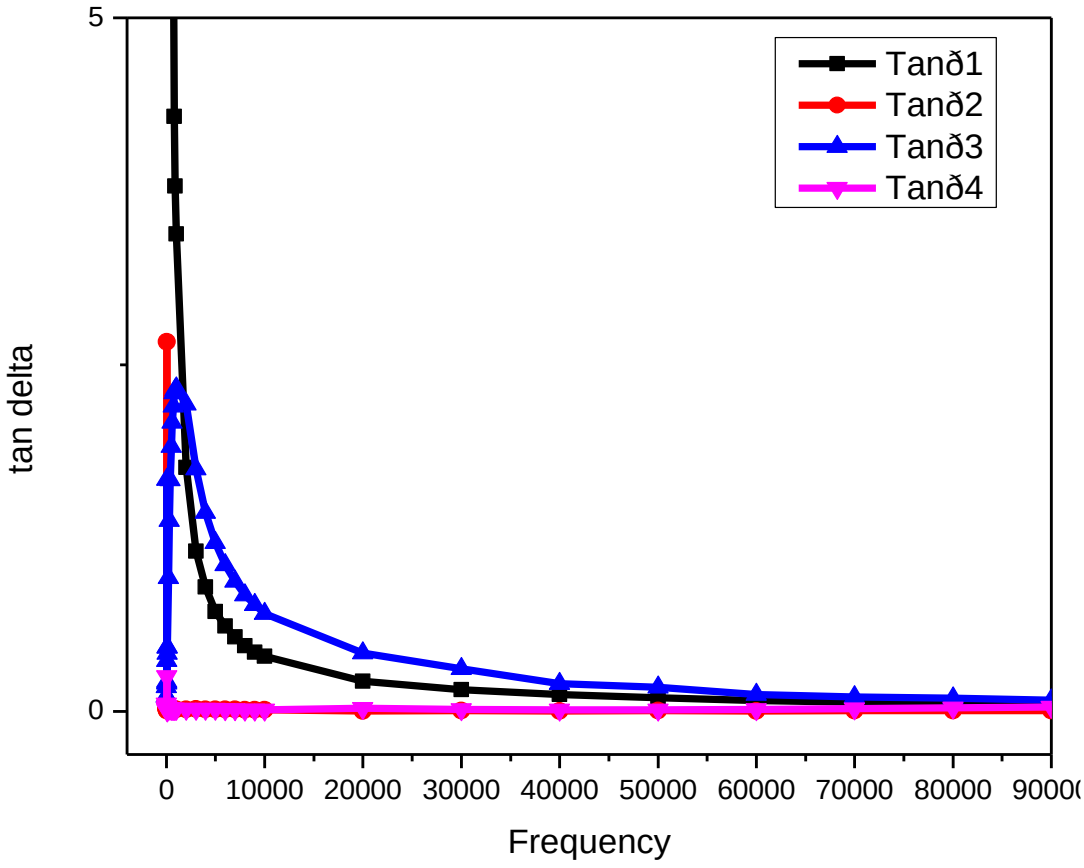

Figure 6. Tandelta Vs Frequency for NiZnFe with rGO.

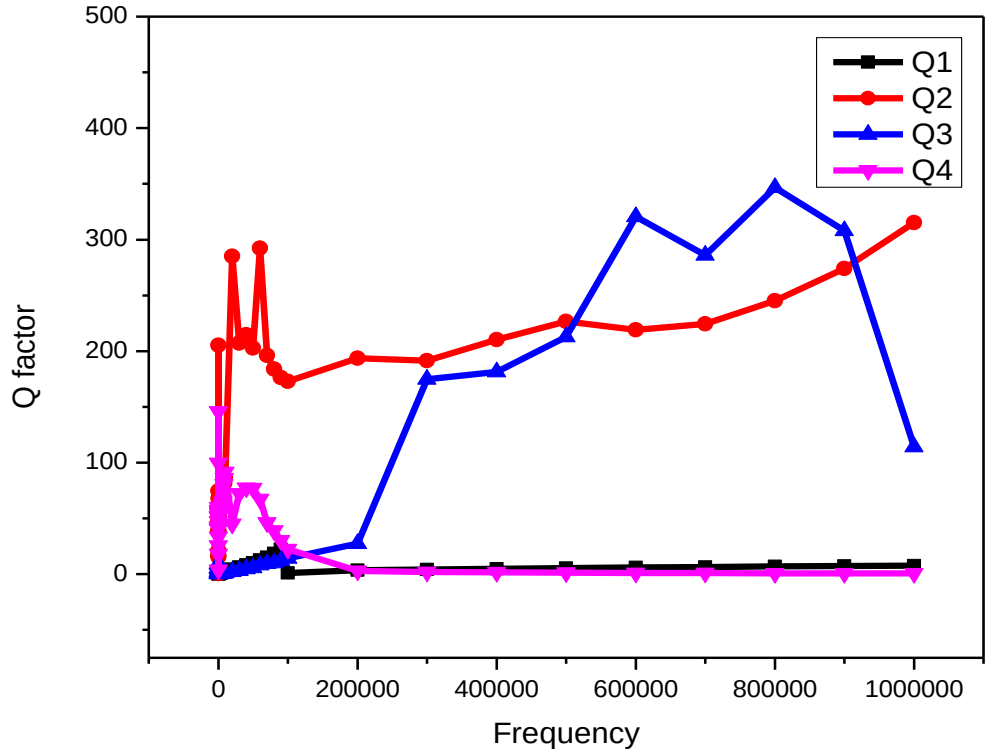

Figure 7. Q factor Vs Frequency for NiZnFe with rGO.

By Maxwell–Wagner–Sillars (MWS) polarization principle, microcapacitors are created when the polarisation of the interfacial regions between the polymer and filler particles that in turn causes an accumulation of charges at the grain boundaries.

The Q factor is inversely proportional to tan δ is given by Eq. (1)

Q = (Energy lost per cycle)/(Energy stored per cycle) (1) [28]

Because of the decreasing oscillations in the improved blend system they exhibit little energy loss, their Q value is larger. The filler dispersion in the polymer mixture may increase the interfacial regions that function as active interfacing regions and reduce energy loss. Low dielectric loss and a high-quality factor (Q) in a composite material make it appropriate for microwave dielectric applications [10, 11]. The basic relationship between the dielectric constant and a substance's permittivity, or capacity to store energy in an electric field caused the dipolar polarisation of the matrix and the decrease in permittivity with increasing frequency [29]. Table 2 denotes Q factor, tandelta and dielectric const. of NiCoFe-rGO epoxy composite.

Highest average dielectric constant was obtained with intermediate concentration, i.e, 0.6 wt.% NiCoFe and 0.4 wt.% rGO. The material dielectric constant is directly related to the average value of grain size [30, 31]. The increase in atomic radii follows Co < Ni < Zn hence, the decrease in loss tangent which is due to the decrease of grain size [32]. The average crystallite size of NiCoFe varies from 30–44 nm [33] and that of NiZnFe were determined to be ~3.75 μm *[34]* An average particle size of 17 nm obtained for NiCoFe when sintered at 1200 ºC reported in our earlier article [35]. The length, width and thickness of rGO are 200 nm, 80 nm, and 0.335 nm respectively [4].

Due to the dispersion of charges at lower frequencies, as seen in the Figure 5, the dielectric loss reduces with increasing frequency while remaining constant at higher frequencies. The primary causes are the polarisation of space charge and the ions' beginning to lag behind the field, which results in a reduction in dielectric loss [31].

Table 4. Average values of Q factor, tandelta and dielectric const. of NiZnFe-rGO epoxy composite

NiZnFe-rGO	Q factor	tandelta	% decrease in dielectric loss	Dielectric constant	% increase in dielectric const.
Sample 1	3.652708	0.219537	87.46	15108180648	99.97
Sample 2	123.6157	0.072194	61.88	3337502.489	2.76
Sample 3	45.64457	0.737444	96.26	63523968.59	94.89
Sample 4	45.65305	0.209951	86.89	3647864.992	11.03
Neat epoxy	426.7927	0.027518		3245277.084	

From Table 4 its observed that a high dielectric constant obtained for higher NiZnFe concentration and the Q factor values increases in the high frequency regime for (0.6 & 0.4 wt.%) of NiZnFe with rGO. The interfaces of the graphene nanoparticles and the concentration of NiZnFe microparticles have an inhibitory influence on the transmission of charges. The polymer dielectrics suffer localised breakdown and additional deterioration as a result of the strong electric field. The lifespan and dependability of the insulation may be considerably extended if the growth of the electrical trees could be prevented [36], which is a result of defects such as voids and impurities.

From Figure 7 for the intermediate concentration, a higher Q factor value obtained in the high frequency for NiZnFe. This could be by the combined effect of micro- and nano-entities that has a significant effect on the enhancement of dielectric properties [36, 37]. The Q factor for higher NiZnFe filler loadings not high compared to the intermediate loadings, this could be by concentration difference in the individual dielectric characteristics of the micro and nano fillers that losses the dipolar motion in composite. The nano particles capture the mobile charges and opposes the partial discharge erosion and also enhance the bonding strength of the polymer but the microparticles covered by nanoparticles improves the interfacial polarization of the entire composite [36].

The production of single or multiple helices or chain breakdown can be used to systematically align the long-range epoxy chains. The helices heads one behind the other thereby the movement of ion transport and conductivity persists though the filler linkages in the broken linkages [14].

The dielectric loss is caused by the energy loss at grain boundaries resulting in the shift in polarization when the material is subjected to an electric field [31, 32]. The dielectric loss happen due to migration of space charge by interfacial polarization and dipolar motion [38].

CONCLUSION

In this work, dielectric properties was explored for nickel cobalt ferrite and nickel zinc ferrite graphene epoxy composite and it was confirmed that enhancement in dielectric constant and decrease in dielectric loss for nickel cobalt ferrite with graphene and a higher dielectric constant obtained in the nickel zinc ferrite graphene composite. At the lower frequency a higher dielectric property obtained and that gradually decreased with increase in the frequency which is due to relaxation of the dipoles present in the polymer blends. The dielectric loss decreases with increasing frequency, due to the dispersion of charges at lower frequencies and polarization of space charges.

Acknowledgments

The authors extend their appreciation to the Researchers supporting project SERB CRG/2022/003429, Govt of India.

REFERENCES

1. A. A. Azeez, K. Y. Rhee, S. J. Park, and D. Hui, “Epoxy clay nanocomposites – processing, properties and applications: A review,” *Compos. Part B Eng.*, vol. 45, no. 1, pp. 308–320, Feb. 2013, doi: 10.1016/j.compositesb.2012.04.012.

2. M. F. Shukur, N. A. Majid, R. Ithnin, and M. F. Z. Kadir, "Effect of plasticization on the conductivity and dielectric properties of starch-chitosan blend biopolymer electrolytes infused with NH4Br," *Phys. Scr.*, vol. T157, 2013, doi: 10.1088/0031-8949/2013/T157/014051.
3. E. Bementa, M. A. Jothi Rajan, and E. S. Gnanadass, "Effect of Prolonged Duration of Gelatinization in Starch and Incorporation with Potassium Iodide on the Enhancement of Ionic Conductivity," *Polym. - Plast. Technol. Eng.*, vol. 56, no. 15, pp. 1632–1645, 2017, doi: 10.1080/03602559.2017.1289392.
4. M. George and A. Mohanty, "Investigation of mechanical properties of graphene decorated with graphene quantum dot-reinforced epoxy nanocomposite," *J. Appl. Polym. Sci.*, vol. 137, no. 19, pp. 1–12, 2020, doi: 10.1002/app.48680.
5. D. W. Tavernier, K., Varlow, B. R. & Auckland, "Electrical tree modelling in non-linear insulation. Conference on Electrical Insulation and Dielectric Phenomena," *Annu. Rep. Atlanta, USA. IEEEe*.
6. G. M. Joshi and K. Deshmukh, "Study of conjugated polymer/graphene oxide nanocomposites as flexible dielectric medium," *J. Mater. Sci. Mater. Electron.*, vol. 27, no. 4, pp. 3397–3409, 2016, doi: 10.1007/s10854-015-4172-z.
7. J. Anandraj and G. M. Joshi, "Fabrication, performance and applications of integrated nanodielectric properties of materials–a review," *Compos. Interfaces*, vol. 25, no. 5–7, pp. 455–489, 2018, doi: 10.1080/09276440.2017.1361717.
8. P. O. Henk, T. W. Kortsen, and T. Kvarts, "Increasing the electrical discharge endurance of acid anhydride cured DGEBA epoxy resin by dispersion of nanoparticle silica," *High Perform. Polym.*, vol. 11, no. 3, pp. 281–296, 1999, doi: 10.1088/0954-0083/11/3/304.
9. L. Sun, R. Zhang, Z. Wang, E. Cao, Y. Zhang, and L. Ju, "Microstructure, dielectric properties and impedance spectroscopy of Ni doped CaCu3Ti4O12 ceramics," *RSC Adv.*, vol. 6, no. 61, pp. 55984–55989, 2016, doi: 10.1039/c6ra07726a.
10. B. Jancar, D. Suvorov, M. Valant, and G. Drazic, "Characterization of CaTiO 3 -NdAlO 3 dielectric ceramics," vol. 23, pp. 1391–1400, 2003.
11. G. Murugesan, R. Nithya, S. Kalainathan, and S. Hussain, "High temperature dielectric relaxation anomalies in Ca0.9Nd0.1Ti0.9Al0.1O3-δ single crystals," *RSC Adv.*, vol. 5, no. 96, pp. 78414–78421, 2015, doi: 10.1039/c5ra15876a.
12. T. John Lewis, "Nano-composite dielectrics: The dielectric nature of the nano-particle environment," *IEEJ Trans. Fundam. Mater.*, vol. 126, no. 11, pp. 1020–1030, 2006, doi: 10.1541/ieejfms.126.1020.
13. B. Hallouet, P. Desclaux, B. Wetzel, A. K. Schlarb, and R. Pelster, "Analysing dielectric interphases in composites containing nano- and micro-particles," *J. Phys. D. Appl. Phys.*, vol. 42, no. 6, 2009, doi: 10.1088/0022-3727/42/6/064004.
14. M. Sabu, E. Bementa, Y. Jaya Vinse Ruban, and S. Ginil Mon, "A novel analysis of the dielectric properties of hybrid epoxy composites," *Adv. Compos. Hybrid Mater.*, vol. 3, no. 3, pp. 325–335, 2020, doi: 10.1007/s42114-020-00166-0.
15. Y. Cheng, G. Yu, B. Yu, and X. Zhang, "The research of conductivity and dielectric properties of ZnO/LDPE composites with different particles size," *Materials (Basel).*, vol. 13, no. 18, 2020, doi: 10.3390/ma13184136.
16. X. Zhang, M. Q. Le, O. Zahhaf, J. F. Capsal, P. J. Cottinet, and L. Petit, "Enhancing dielectric and piezoelectric properties of micro-ZnO/PDMS composite-based dielectrophoresis," *Mater. Des.*, vol. 192, p. 108783, 2020, doi: 10.1016/j.matdes.2020.108783.
17. D. C. Marcano *et al.*, "Improved Synthesis of Graphene Oxide," *ACS Nano*, vol. 4, no. 8, pp. 4806–4814, Aug. 2010, doi: 10.1021/nn1006368.
18. N. V. Lakshmi and P. Tambe, "EMI shielding effectiveness of graphene decorated with graphene quantum dots and silver nanoparticles reinforced PVDF nanocomposites," *Compos. Interfaces*, vol. 24, no. 9, pp. 861–882, 2017, doi: 10.1080/09276440.2017.1302202.
19. K. Maaz, W. Khalid, A. Mumtaz, S. K. Hasanain, J. Liu, and J. L. Duan, "Magnetic characterization of Co1-xNixFe2O4 (0≤x≤1) nanoparticles prepared by co-precipitation route," *Phys. E Low-Dimensional Syst. Nanostructures*, vol. 41, no. 4, pp. 593–599, 2009, doi:

10.1016/j.physe.2008.10.009.
20. P. S. Anil Kumar, J. J. Shrotri, S. D. Kulkarni, C. E. Deshpande, and S. K. Date, "Low temperature synthesis of Ni0.8Zn0.2Fe2O4 powder and its characterization," *Mater. Lett.*, vol. 27, no. 6, pp. 293–296, 1996, doi: 10.1016/0167-577X(96)00010-9.
21. R. Yang *et al.*, "Fabrication of NiCo2-Anchored Graphene Nanosheets by Liquid-Phase Exfoliation for Excellent Microwave Absorbers," *ACS Appl. Mater. Interfaces*, vol. 9, no. 14, pp. 12673–12679, 2017, doi: 10.1021/acsami.6b16144.
22. M. M. Rashad, E. M. Elsayed, M. M. Moharam, R. M. Abou-Shahba, and A. E. Saba, "Structure and magnetic properties of NixZn1-xFe2O4 nanoparticles prepared through co-precipitation method," *J. Alloys Compd.*, vol. 486, no. 1–2, pp. 759–767, 2009, doi: 10.1016/j.jallcom.2009.07.051.
23. C. Singh, A. Goyal, and S. Singhal, "Nickel-doped cobalt ferrite nanoparticles: Efficient catalysts for the reduction of nitroaromatic compounds and photo-oxidative degradation of toxic dyes," *Nanoscale*, vol. 6, no. 14, pp. 7959–7970, 2014, doi: 10.1039/c4nr01730g.
24. B. J. C., "Ferroelectrics: An Introduction to the Physical Principles.," *Van Nostrand-Reinbold, London.*.
25. E. Dhanumalayan and S. Kaleemulla, "Enhanced structure, dielectric, and thermal properties of attapulgite clay and hexagonal boron nitride admixture loaded polymer blends," *J. Mater. Sci. Mater. Electron.*, vol. 31, no. 20, pp. 17828–17842, 2020, doi: 10.1007/s10854-020-04337-z.
26. E. Dhanumalayan and G. M. Joshi, "Quality factor of potassium hexa-titanate oxide ceramic reinforced polymer blends for broad band applications," *AIP Conf. Proc.*, vol. 1992, 2018, doi: 10.1063/1.5047957.
27. Ahmad Z., "Polymer dielectric materials," *Dielectr. Mater. (IntechOpen, London)*.
28. Liang E.C., "Microwave J.," vol. 58(2), p..
29. J. C. H. Koh, Z. A. Ahmad, and A. A. Mohamad, "Bacto agar-based gel polymer electrolyte," *Ionics (Kiel).*, vol. 18, no. 4, pp. 359–364, 2012, doi: 10.1007/s11581-011-0631-6.
30. P. Nayak, T. Badapanda, A. K. Singh, and S. Panigrahi, "An approach for correlating the structural and electrical properties of Zr4+-modified SrBi4Ti4O15/SBT ceramic," *RSC Adv.*, vol. 7, no. 27, pp. 16319–16331, 2017, doi: 10.1039/c7ra00366h.
31. C. Rayssi, S. El Kossi, J. Dhahri, and K. Khirouni, "Frequency and temperature-dependence of dielectric permittivity and electric modulus studies of the solid solution Ca0.85Er0.1Ti1-: XCo4 x /3O3 ($0 \leq x \leq 0.1$)," *RSC Adv.*, vol. 8, no. 31, pp. 17139–17150, 2018, doi: 10.1039/c8ra00794b.
32. C. Rayssi, F. I. H. Rhouma, J. Dhahri, K. Khirouni, M. Zaidi, and H. Belmabrouk, "Structural, electric and dielectric properties of Ca0.85Er0.1Ti1−xCo4x/3O3($0 \leq x \leq 0.1$)," *Appl. Phys. A Mater. Sci. Process.*, vol. 123, no. 12, pp. 1–13, 2017, doi: 10.1007/s00339-017-1365-8.
33. N. B. Velhal, N. D. Patil, A. R. Shelke, N. G. Deshpande, and V. R. Puri, "Structural, dielectric and magnetic properties of nickel substituted cobalt ferrite nanoparticles: Effect of nickel concentration," *AIP Adv.*, vol. 5, no. 9, 2015, doi: 10.1063/1.4931908.
34. A. C. Hee, I. H. S. C. Metselaar, M. R. Johan, and M. Mehrali, "Preparation of Nickel Zinc Ferrite by Electrophoretic Deposition," *J. Electrochem. Soc.*, vol. 159, no. 1, pp. E18–E22, 2011, doi: 10.1149/2.068201jes.
35. M. George *et al.*, "Thermal and magnetic properties study of NiCo2O4/graphene and NiFe2O4/graphene," *Mater. Today Proc.*, vol. 72, no. xxxx, pp. 2921–2927, 2023, doi: 10.1016/j.matpr.2022.07.457.
36. W. Wang and Y. Yang, "The Synergistic Effects of the Micro and Nano Particles in Micro-nano Composites on Enhancing the Resistance to Electrical Tree Degradation," *Sci. Rep.*, vol. 7, no. 1, pp. 1–10, 2017, doi: 10.1038/s41598-017-08761-w.
37. Y. Tang *et al.*, "Temperature effects on the dielectric properties and breakdown performance of h-BN/epoxy composites," *Materials (Basel).*, vol. 12, no. 24, 2019, doi: 10.3390/ma1224112.
38. K. Yang, X. Huang, Y. Huang, L. Xie, and P. Jiang, "Polymerization : Toward Ferroelectric Polymer Nanocomposites with," *Chem. Mater.*, vol. 25, pp. 2327–2338, 2013.

